Differential Interactions of Estrogens and Antiestrogens at the 17β-Hydroxyl or Counterpart Hydroxyl with Histidine 524 of the Human Estrogen Receptor α[†]

Sigrid Aliau, Hélène Mattras, Eric Richard, Jean-Claude Bonnafous, and Jean-Louis Borgna*

INSERM U.439, 70 rue de Navacelles, 34090 Montpellier, France

Received December 26, 2001; Revised Manuscript Received April 5, 2002

ABSTRACT: We investigated the role of H524 of the human estrogen receptor α (ERα) for the binding of various estrogens [estradiol (E_2), 3-deoxyestradiol (3-dE_2), and 17β-deoxyestradiol (17β-dE_2)] and antiestrogens [4-hydroxytamoxifen (OHT), RU 39 411 (RU), and raloxifene (Ral)], which possess the 17β-hydroxyl or counterpart hydroxyl (designated: 17β/c-OH), with the exception of 17β-dE_2 and OHT. The work involved a comparison of the binding affinities of these ligands for wild-type and H524 mutant ERs, modified or not with diethyl pyrocarbonate (DEPC), a selective histidine reagent. Alanine substitution of H524 did not significantly change the association affinity constant (relative to OHT) of 17β-dE_2, whereas those of RU, Ral, E_2, and 3-dE_2 were decreased 3-fold, 14-fold, 24-fold, and 49-fold, respectively. Values of the two ligands available in radiolabeled form (E_2 and OHT) were correlated with the dissociation rate constants, which were increased 250-fold and 2-fold, respectively. The action of DEPC on wild-type ER led to a homogeneous ER population which still bound antiestrogens and 17β-dE_2 with practically unchanged affinities (less than 4-fold decreases in relative affinity constants), while E_2 and 3-dE_2 displayed markedly decreased affinities (56-fold decrease for E_2). Conversely, DEPC treatment of H524A mutant ER did not induce marked decreases in the relative affinities of any of the checked compounds (decreases $\leq$3-fold). All of these effects appeared to involve H524 as the H516A mutant behaved as wild-type ER. These combined data relative to mutated or DEPC-modified ER converged to support that the interaction of 17β/c-OH of ER ligands with H524 is strong for estrogens and weaker for antiestrogens, with quantitative or qualitative differences between the binding modes of the latter, as illustrated by RU and Ral. The abilities of E_2 and OHT to protect the various ER types against inactivation by DEPC were strikingly different: OHT totally prevented the effect of DEPC on wild-type, H516A, and H524A ERs, while E_2 only partially protected wild-type and H516A ERs (H516A ER > wild-type ER) and very weakly protected H524A ER. Molecular modeling was tentatively used to interpret the biochemical results.

Estrogens play important roles in a large array of physiological processes such as development, sexual differentiation, and reproduction (*1*), and are also involved in pathological processes, especially the promotion and growth of most breast cancers (*2*). In mammals, the biological activity of estrogens is mediated mainly at the transcriptional level by two estrogen receptors (ERα[1] and ERβ), which belong to the nuclear receptor superfamily (*3*, *4*), a class of ligand-inducible transcription factors. ERα, which is the predominating ER form in major estrogen target organs such as uterus (*5*, *6*), was cloned from human cells in 1985 (*7*, *8*), whereas ERβ was more recently identified in human (*9*) and rat (*10*) tissues. As other nuclear receptor superfamily members, each of the two proteins includes two evolutionarily conserved functional domains, i.e., the DNA-binding domain and the ligand-binding domain (LBD).

To interpret the estrogenic or antiestrogenic properties of ER ligands on a rational basis, and to design new selective ER modulators, it is crucial to dissect the molecular mechanisms of ER/ligand recognition and their incidence on coactivator or corepressor recruitment. In recent years, a number of crystallographic data related to various LBD/ligand complexes (*11*) has considerably improved our knowledge in this field. The crystal structures of unmodified or cysteine S-carboxymethylated human ERα (*12*−*15*) and ERβ (*16*, *17*) LBDs bound to estrogen or antiestrogen were recently established. Brzozowski et al. (*12*) first reported structures of ERα LBD bound to estradiol (E_2) and raloxifene (Ral), a partial agonist/antagonist; then Shiau et al. (*14*) described structures of LBD bound to diethylstilbestrol, a *trans*-stilbene estrogen, and 4-hydroxytamoxifen (OHT), another partial agonist/antagonist (Figure 1). The overall architecture of the ERα LBD is similar to those determined for other nuclear receptor LBDs (*18*). It includes 12 α-helices and 1 β-sheet and is folded into a 3-layered antiparallel α-helical sandwich. Agonists and antagonists bind to the same site, defined as the ligand-binding pocket (LBP), within the LBD core and show several common binding features:

[†] This work was supported by the Institut National de la Santé et de la Recherche Médicale and the Association pour la Recherche sur le Cancer.

* To whom correspondence should be addressed (Tel: 33 4 67 04 37 14, Fax: 33 4 67 04 37 15, E-mail: Borgna@u439.montp.inserm.fr).

[1] Abbreviations: ER, estrogen receptor; LBD, ligand-binding domain; LBP, ligand-binding pocket; E_2, estradiol; 3-dE_2, 3-deoxyestradiol; 17β-dE_2, 17β-deoxyestradiol; OHT, 4-hydroxytamoxifen; Ral, raloxifene; RU, RU 39 411; 17β/c-OH, 17β or counterpart hydroxyl; DEPC, diethyl pyrocarbonate; P50, 50 mM sodium phosphate buffer, pH 7; PBS, phosphate-buffered saline; RAC, relative affinity constant.

10.1021/bi0121914 CCC: $22.00
Published on Web 06/01/2002

E353, in helix 3 [the ERα helix numbering of Brzozowski et al. (*12*) will be used], and R394, in helix 6, are directly involved in hydrogen bonding of the phenolic OH common to all estrogens and antiestrogens; H524, in helix 11, is involved in a single hydrogen bond with 17β-OH of E_2 (or the second phenolic OH of diethylstilbestrol or Ral). The N atom of Ral or OHT is involved in a salt bridge with D351.

Alanine scanning mutagenesis was used to identify amino acids in the 515−535 region of ERα LBD that are important for ligand binding or promoting ER-induced transcription (*19, 20*). Four ligands were used for these investigations: the three estrogens E_2, hexestrol, and zearalenone (two nonsteroidal estrogens possessing the two OHs homologous to the phenolic OH and 17β-OH of E_2) and the antiestrogen OHT. The authors found that alanine substitution of L525 had a unique deleterious effect on the ability of the four compounds to activate ER, whereas alanine substitution at a neighbor amino acid, H524, had a simular pronounced deleterious effect on the three estrogen actions but had no effect on that of OHT.

In previous studies (*21, 22*), we observed that treatment of sheep uterine ER (essentially ERα) by diethyl pyrocarbonate (DEPC), a reagent which reversibly modifies histidine and tyrosine residues, differentially affected the recognition of estrogens and antiestrogens possessing 17β-OH (steroidal ligands) or counterpart hydroxyl (nonsteroidal ligands).

The results of crystallographic, alanine scanning mutagenesis, and DEPC-modification studies suggested that in ER LBP the environment of the antiestrogen 17β-OH or counterpart hydroxyl (17β/c-OH) differs from that of estrogens. In light of these results, the purpose of the present work was to provide additional information on the involvement of H524 in the binding of various ligands to ERα. We first compared the relative affinities of E_2, its two monodeoxy forms (3-dE_2 and 17β-dE_2), and antiestrogens possessing (Ral and RU) or not (OHT) 17β/c-OH (Figure 1) for wild-type and H524A human ERs. We then studied the effect of DEPC on the ability of wild-type and mutant ERs to bind E_2 and OHT and evaluated the capacity of these two ligands to protect ER LBD against DEPC inactivation. Finally, we assessed variations in the relative affinities of the above-mentioned estrogens and antiestrogens upon DEPC-modification of wild-type and H524A ERs. The results obtained by the various approaches indicate that H524 is differentially involved in the binding of estrogens and antiestrogens possessing 17β/c-OH. Using crystal structures of human ERα LBD bound to E_2, Ral (*12*), or OHT (*14*) as templates, molecular modeling was tentatively applied to interpret the binding data obtained with wild-type and H524A ERs.

EXPERIMENTAL PROCEDURES

Materials. pCMV5 plasmids coding for wild-type human ERα and the two H516A and H524A mutants were given by B. S. Katzenellenbogen; preparation of these plasmids has been previously described (*19*). [6,7-^{3}H]E_2 (1.78 PBq/mol, 99% radiochemical purity) was purchased from NEN Life Science Products. *Z*-[*N-methyl*-^{3}H]OHT (3.00 PBq/mol, 73% original radiochemical purity) was purchased from Amersham Pharmacia Biotech; radioactive contaminants (*E*-[*N-methyl*-^{3}H]OHT and mainly the *N*-oxide forms of *Z*- and *E*-[*N-methyl*-^{3}H]OHT) were separated from *Z*-[*N-methyl*-^{3}H]-OHT by thin-layer chromatography on analytical silical gel plates using chloroform−piperidine (9:1) as eluent. The purity of tritiated OHT used for binding studies was >95%. E_2, 3-dE_2, 17β-dE_2, and RU were donated by Aventis (Romainville, France); OHT was provided by Zeneca Pharmaceuticals (Macclesfield, England) and Ral by Lilly Research Laboratories (Indianapolis, IN). DEPC and histidine were purchased from Sigma Aldrich. Ethanolic solutions of radioactive and radioinert ligands were stored at −20 °C. The compound purity was checked before use by thin-layer chromatography. All other reagents were analytical grade.

ER Expression and Extraction. COS-7 cells were grown in Dulbecco's modified Eagle's tissue culture medium supplemented with 10% fetal calf serum, penicillin (100 units/mL), and streptomycin (100 μg/mL). Nearly confluent cells were trypsinized, harvested, and washed in phosphate-buffered saline (PBS), and then in PBS−Optimem (Gifco-BRL) (2:1). Cells were resuspended in Optimem (10^8 cells/mL) and supplemented with 2 volumes of 40 mM $MgSO_4$, 50 mM K_2PO_4H, 20 mM CH_3CO_2K, 20 mM KOH (pH 7.4), 20 μg of carrier plasmid (pSG5), and 2 μg of expression plasmid (pCMV5) coding for wild-type or mutant ER. After 20 min on ice, 0.3 mL aliquots were distributed in electroporation cuvettes and electroporated at 960 μF and 280 V. Cells were collected in normal growth medium and distributed in 150 mm dishes (5×10^6 cells/dish). After adherence, cells were washed twice with PBS and further grown for 48 h in phenol red-free tissue culture medium, supplemented with 5% charcoal−dextran-treated fetal calf serum, penicillin, and streptomycin. Cells were trypsinized and then harvested; they were washed twice in PBS, resuspended in 50 mM sodium phosphate, pH 7, buffer (P50), and disrupted by sonication. The homogenate was then centrifuged at $10^5 g$ for 30 min at 4 °C. Aliquots of supernatants were used for determination of protein concentration, according to Bradford (*23*), and ER concentration (cf. *Ligand-Binding Assays*). Cytosol samples were frozen and stored in liquid nitrogen. For binding studies, aliquots were thawed and ER concentrations adjusted to ∼1−4 nM by dilution with P50. When necessary, bovine serum albumin was added to diluted cytosol to reach a final protein concentration of at least 1 mg/mL to avoid nonspecific ER adsorption to charcoal in the binding assays.

ER Modification by DEPC. Aliquots of cytosol containing wild-type, H516A, or H524A ER were preincubated or not for 15 h at 0 °C with [^{3}H]E_2 or [^{3}H]OHT in the absence and presence of an excess of the corresponding unlabeled ligand (cf. *Ligand-Binding Assay*s). They were then treated for 30 min at 0 °C, under agitation, with 1% (v/v) freshly prepared ethanol solutions of DEPC. The reaction was stopped by the addition of at least 3-fold excess (relative to DEPC concentrations) of histidine (0.3 M in P50). [^{3}H]E_2 and [^{3}H]OHT binding was then determined by charcoal assays.

Ligand-Binding Assays. Samples of control or DEPC-treated cytosol containing wild-type or mutant ER were incubated for 15 h at 0 °C with 5 nM [^{3}H]E_2 (wild-type and H516A ERs), 20 nM [^{3}H]E_2 (H524A ER), or 5 nM [^{3}H]-OHT (wild-type and mutant ERs), in the absence and presence of 2 μM of the corresponding unlabeled ligand to measure total (B_1) and nonspecific (B_2) concentrations of bound radioligand. Aliquots were then treated with an equal volume of a charcoal suspension (1% charcoal, 0.1% dextran

T_{70} in P50) for 30 min at 0 °C (this time was reduced to 5 min for the measurement of [^{3}H]E_2 binding to H524A ER) and then centrifuged at 4000*g* for 2 min at 0 °C to pellet the charcoal. The specific binding of labeled ligand (B_s) was calculated according to Blondeau and Robel (*24*) from B_1, B_2, and total concentration of radioligand (T):

$$B_s = (B_1 - B_2)\frac{T}{T - B_2}$$

Competitive Binding Assays; Determination of RACs. Competitive binding assays for native and DEPC-modified wild-type, H516A, or H524A ERs were carried out at 20 °C, with 20 h incubation times, as previously described (*21*), using 5 nM [^{3}H]E_2 (native wild-type and H516A ERs), 20 nM [^{3}H]E_2 (native H524A ER), or 5 nM [^{3}H]OHT (native and DEPC-modified ERs) as tracer ligand and increasing concentrations of estrogens and antiestrogens. The binding of [^{3}H]E_2 or [^{3}H]OHT in the samples was determined by charcoal assays. Apparent equilibrium association constants of competitors (K_a^C) relative to those of E_2 or OHT (K_a^H) were calculated from the concentrations of unlabeled E_2 or OHT (*H*) and competitor (*C*) which inhibited [^{3}H]E_2 or [^{3}H]-OHT specific binding to the same extent, according to Korenman (*25*):

$$\mathrm{RAC} = \frac{K_a^{\,C}}{K_a^{\,H}} = \frac{\dfrac{H_t^* - H_b^*}{H_{sb}^*} \cdot \dfrac{H}{C}}{\dfrac{H_t^* - H_b^*}{H_{sb}^*} + 1 - \dfrac{H}{C}}$$

H_t^* is the total concentration of radioligand; H_b^* and H_{sb}^* are the respective concentrations of bound and specifically bound radioligand; $H_t^* - H_b^*$ was assumed to be the unbound labeled ligand concentration. RACs were routinely determined using 50% inhibition conditions. They were expressed as the percent of OHT affinities for the various native or DEPC-modified ERs.

Dissociation Kinetics. Samples of cytosol containing wild-type, H516A, or H524A ER, pretreated or not with DEPC, were incubated for 15 h at 0 °C or for 1 h at 20 °C with 5 nM [^{3}H]E_2 (native wild-type and H516A ERs), 20 nM [^{3}H]-E_2 (native H524A ER), or 5 nM [^{3}H]OHT (native and DEPC-modified ERs), in the presence of 2 μM corresponding radioinert ligand for nonspecific binding determination. Radioligand dissociation was initiated by adding 1% of 0.1 mM ethanolic solutions of radioinert E_2 or OHT. At different times, aliquots were treated with charcoal for 30 min at 0 °C (5 min for [^{3}H]E_2 binding to H524A ER) and then centrifuged at 4000*g* for 2 min to determine radioligand binding. The specific binding of [^{3}H]E_2 or [^{3}H]OHT was calculated as described above (cf. *Ligand-Binding Assays*).

Molecular Mechanics Studies. All energy minimization and molecular dynamics simulations with ERα LBD models were performed using the InsightII/Discover software from MSI, and CFF91 as force field.

(A) Building of a Complete ER LBD/Ral Complex. The starting X-ray crystallographic structure of the human ERα LBD/Ral complex (entry 1ERR in the Protein DataBank; monomer A) (*12*) was lacking the loop sequences 460−469 (helix 9−helix 10 loop) and 529−534 (helix 11−helix 12 loop). Moreover, several poorly resolved amino acid residues were not specified. The two lacking sequences were imported from the crystallographic structure of the ERα LBD/OHT complex (entry 3ERT in the Protein DataBank; monomer A) (*14*), and lacking amino acid side chains were introduced in the complex. All water molecules from the crystallographic structure were deleted with the exception of the one involved in hydrogen bonding of the Ral benzothiophene OH moiety. The resulting complete LBD/Ral complex was minimized (no restraint on the added structural elements, all other α-carbons fixed).

(B) Conformational Analysis of RU and Its Docking into ER LBD. The conformational search was performed using the Monte Carlo method. The lowest energy structure of RU was selected for docking of its steroidal portion into the LBD structure. It was achieved by superimposing RU to Ral, so as to obtain optimal overlap of the two ligands: coincidence of RU 3-O with benzothiophene-linked O of Ral and tight proximity of RU 17β-O with the second phenolic O of Ral. Chemical bond rotations inside the RU 11β-substituent allowed optimization of the overlap with its Ral homologue, with very close locations of N atoms. After Ral deletion, steric clashes between RU and LBD were manually suppressed by appropriate rotations of some side chains. A first minimization was carried out with fixed LBD α-carbons, except those of helix 7−helix 8 and helix 11−helix 12 loops (which are close to LBP and therefore liable to participate in the ER adaptation to the ligand structure), and constrained interactions between: (i) the RU 3-OH with E353 and R394 side chains and with the bound water molecule, (ii) the RU 17β-OH with the H524 imidazole ring, and (iii) the RU $N(CH_3)_2$ with D351. A second round of minimization was performed as indicated above except that the LBD/ligand interaction constraints were suppressed. The minimized complex was submitted to molecular dynamics simulation (5 ps temperature increase and 200 ps heating at 300 K; dielectric constant value: 1). All checked conformational states of the complex appeared to be very similar after minimization (RMSD lower than 1.0 Å). The lowest energy structure was selected for matching with the crystallographic structures of LBD/ligand complexes, more specifically to check possible variations in H524 positioning.

RESULTS

As the affinities of the reference ligands [^{3}H]E_2 and [^{3}H]-OHT are considerably underestimated when measured by equilibrium analysis (*26*), competition binding experiments cannot result in accurate K_i determinations for the various unlabeled estrogens or antiestrogens. We thus only used such experiments to the determination of relative affinity constants (RACs) for each ER type. However, we measured the kinetic dissociation rates of the two tritiated ligands, as they are assumed to predominantly govern their equilibrium constants relative to the bimolecular process of their interactions with ERs (*27*).

RACs of Estrogens and Antiestrogens for Wild-Type, H516A, and H524A ERs. We assessed the importance of the ERα H524 residue in the binding of steroidal or nonsteroidal ligands, possessing 17β/c-OH or not. We determined the RACs of three estrogens (E_2, 3-dE_2, and 17β-dE_2) and three antiestrogens (OHT, Ral, and RU) (Figure 1) for wild-type

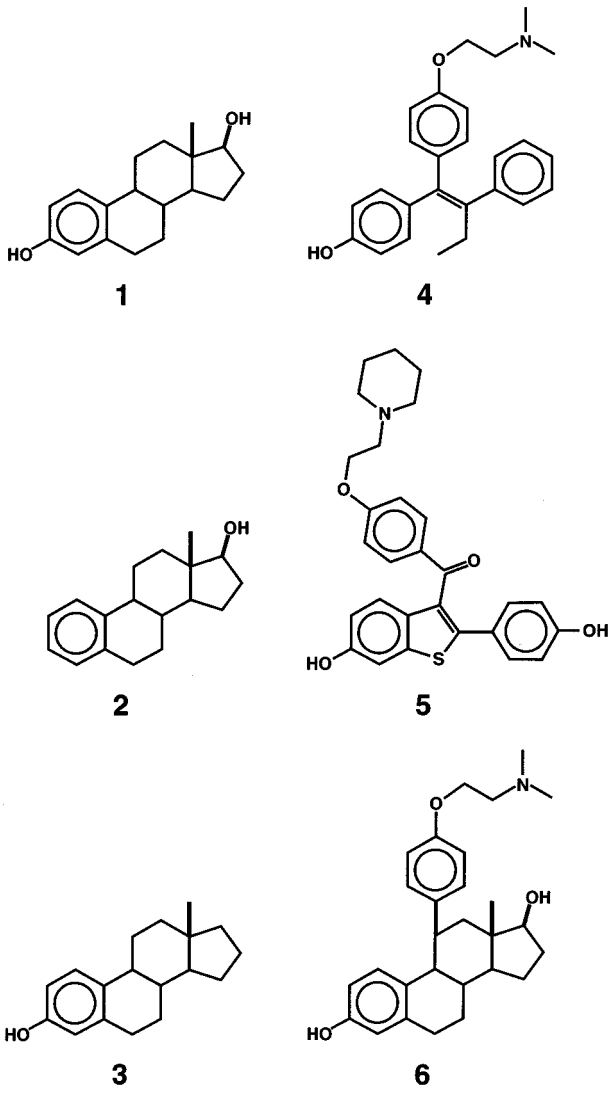

FIGURE 1: Structures of estrogens and antiestrogens used in this study. The three estrogens, estradiol (E_2) **1** and its two monodeoxy forms, 3-deoxyestradiol (3-dE_2) **2** and 17β-deoxyestradiol (17β-dE_2) **3**, and the three antiestrogens, 4-hydroxytamoxifen (OHT) **4**, raloxifene (Ral) **5**, and RU 39 411 (RU) **6**, are shown. Note that (i) except for **2**, all compounds include the phenol of E_2 or its counterpart in nonsteroidal compounds **4** and **5** [for the latter, the counterpart of the E_2 phenol is the benzothiophene phenol (*12*)]; and (ii) like E_2, compounds **2** and **6** possess 17β-OH and compound **5** possesses a phenolic OH counterpart (second phenol group) whereas compounds **3** and **4** are devoid of 17β-OH or counterpart.

and H524A ERs (or H516A ER as control) transiently expressed in COS cells. The results of competitive binding experiments between [^{3}H]OHT or [^{3}H]E_2 and the six unlabeled ligands are given in Table 1. For wild-type ER, the RACs of the three antiestrogens were much higher than those of the three estrogens with the following decreasing affinity order: OHT > RU > Ral > E_2 > 17β-dE_2 > 3-dE_2. The E_2 RAC was found to be 3-fold higher and 123-fold higher than that of 17β-dE_2 and 3-dE_2, respectively, whereas it was 13-fold lower than that of OHT. RU, Ral, and 17β-dE_2 RACs were similar to those determined for the sheep uterine ER (*22*), whereas those of 3-dE_2, and especially E_2, were 7-fold and 28-fold lower, respectively. These discrepancies suggested that 17β-OH is involved in differential estrogen recognition by human and sheep ERαs. Alanine substitution of H524 induced a decrease in all compound RACs, with the exception of 17β-dE_2 which is the only OHT competitor deprived of 17β/c-OH. However, decreases in RAC values markedly varied with compounds: 3-fold for RU, 14-fold for Ral, 24-fold for E_2, and 49-fold for 3-dE_2. It is noteworthy that the E_2 affinity for H524A ER appeared to be 9-fold lower and 303-fold lower than that of 17β-dE_2 and OHT, respectively. The low affinity of E_2 for H524A ER was also revealed by direct binding experiments: a much higher E_2 concentration was required to obtain a given extent of H524A ER saturation as compared to wild-type ER (cf. Figure 3). To verify the specificity of the effect of the H524A substitution on ligand recognition, we determined the ligand RACs for H516A ER. This mutant ER was used as a control because in crystallized LBD, H516 was the nearest histidine to H524, located about two turns from the latter in helix 11 (*12*). The H516A ER displayed almost unchanged RACs for all tested ligands, as compared to wild-type ER (Table 1); only 2-fold and 3-fold decreases were observed for E_2 and 3-dE_2, respectively.

Dissociation Rates of E_2 and OHT from Wild-Type and Mutant ERs. The two ligands E_2 and OHT dissociated from wild-type and mutant ERs according to binary processes (Figure 2). The minor component, the extent of which depends on the ligand and ER type complex, corresponded to fast-dissociating complexes; the major component corresponded to slower dissociating complexes, whose dissociation occurred according to quasi-first-order processes. At 20 °C, the mean half-dissociation times of E_2 from wild-type (Figure 2B) and H516A ERs were 2-fold and 4-fold lower than those of OHT (Table 2); these values only partially reflected the differences in RACs of the two ligands shown in Table 1. In contrast, alanine substitution of H524 differentially affected the dissociation kinetics of the two ligands; the half-dissociation time of OHT (Figure 2D) was little affected while that of E_2 was extremely shortened ($\ll$5 min). To more accurately compare the half-dissociation times of the two ligands, dissociation kinetics were also performed at 0 °C: the half-dissociation time of E_2 from H524A ER (Figure 2C) was 250-fold lower than that determined for wild-type ER (Figure 2A) and 267-fold lower than the half-dissociation time of OHT (not shown) from the same ER mutant.

Taken together, the results of competition and dissociation experiments indicated that the H524A substitution (i) does not appreciably affect the ER binding of OHT and 17β-dE_2, the two ligands devoid of 17β/c-OH, and (ii) specifically decreases the binding of ligands possessing 17β/c-OH, with a slight effect for RU and more pronounced effects for Ral, and to a greater extent, E_2 and 3-dE_2.

Effect of DEPC on Unliganded Wild-Type and Mutant ERs. The substantial decrease in the affinity of estrogens bearing 17β/c-OH upon H524A substitution in human ER was reminiscent of previous observations concerning the modification of sheep uterine ER by DEPC (*22*). Since at neutral pH the reagent mainly reacts with histidine residues, it seemed interesting to analyze the binding of estrogens and antiestrogens to DEPC-modified wild-type, and mutant ERs. Pretreatment of COS cell extracts (0 °C, pH 7), containing unliganded wild-type, H516A, or H524A ER, with DEPC resulted, as observed with sheep uterine cytosol (*21*), in a rapid decrease in their E_2 or OHT specific binding activities. Saturation analysis experiments were performed to dissect

Table 1: RACs of Ligands for Wild-Type, H524A, and H516A ERs

	RAC[a]			RAC ratio[d]	
ligand	WT	H524A	H516A	H524A/WT	H516A/WT
OHT	100[b]	100[b]	100[b]	1	1
Ral	37 ± 4[c]	2.6 ± 0.3[b]	32 ± 8[c]	0.070	0.86
RU	51 ± 23[c]	20 ± 3[b]	57 ± 5[c]	0.39	1.1
E_2	7.9 ± 0.9[b]	0.33 ± 0.06[b]	3.6 ± 1.0[b]	0.042	0.46
3-dE_2	0.064 ± 0.025[c]	0.0013 ± 0.0002[c]	0.019 ± 0.003[c]	0.020	0.30
17β-dE_2	2.7 ± 0.5[c]	2.9 ± 1.1[c]	3.4 ± 1.2[c]	1.1	1.3

[a] RACs of ligands for wild-type, H524A, and H516A ERs were determined by competitive binding radiometric assays using either [^{3}H]OHT or [^{3}H]E_2 as tracer, as described under Experimental Procedures. Data given are means ± SD from 4−6 independent determinations. [b] Values determined using exclusively [^{3}H]OHT as tracer. [c] Values determined using either [^{3}H]OHT or [^{3}H]E_2 as tracer. [d] Ratios of the mean RAC values of compounds for mutant (H524A or H516A) and wild-type ERs.

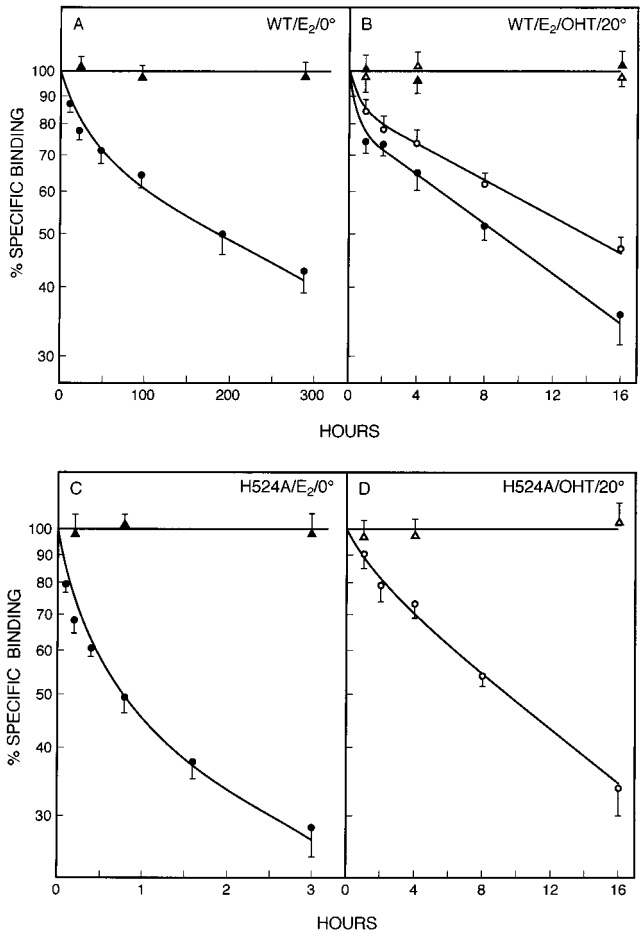

FIGURE 2: Dissociation kinetics of E_2 and OHT from wild-type and H524A ERs. Aliquots of COS extracts containing wild-type (A and B) or H524A (C and D) ER were incubated for 15 h at 0 °C (A and C) or for 1 h at 20 °C (B and D) with [^{3}H]E_2 or [^{3}H]-OHT, as described under Experimental Procedures. The stability and dissociation of [^{3}H]E_2 and/or [^{3}H]OHT at 0 or 20 °C at various times were determined by charcoal assays. The saturable binding of [^{3}H]E_2 (▲, ●) and/or [^{3}H]OHT (△, ○) is plotted as a percentage of the corresponding binding at time 0. (▲, △) Saturable binding of labeled ligands in the absence of the corresponding radioinert ligand; (●, ○) saturable binding of labeled ligands in the presence of the corresponding radioinert ligand. Values are means of duplicate determinations; error bars indicate standard deviations.

the DEPC-induced decreases in the ligand-binding activities of extracts. As shown in Figure 3, DEPC action led to a progressive decrease in the ligand-binding capacities of ERs, which was more marked for E_2 (∼80% to ∼90% decrease induced by 4 mM DEPC) than for OHT (∼50% to ∼60% decrease, respectively). The apparent affinities of OHT for

Table 2: Half-Dissociation Times of E_2 and OHT from Wild-Type, H524A, and H516A ERs[a]

	0 °C		20 °C	
receptor	E_2	OHT	E_2	OHT
wild-type	220 ± 34	ND	8.6 ± 2.7	13.2 ± 2.9
H524A	0.88 ± 0.12	235 ± 59	≪0.1	9.1 ± 1.9
H516A	ND	ND	2.1 ± 0.5	9.3 ± 2.4

[a] Dissociation kinetics of [^{3}H]E_2 and [^{3}H]OHT from wild-type, H524A, and H516A ERs were performed at 0 or 20 °C, as described under Experimental Procedures. Global half-dissociation times (h) were determined by interpolation to the 50% value on curves representing the percentage of specific binding (logarithmic scale) according to the dissociation time. Data given are means ± SD from 2−5 independent determinations. ND: not determined.

the remaining binding sites in DEPC-treated ERs were practically unchanged, whereas they were ∼2-fold lower for E_2. DEPC pretreatment of wild-type and H524A ERs moderately lowered (from ∼3- to ∼7-fold) the half-dissociation times of OHT (not shown). These results indicated that the action of DEPC on wild-type and mutant ERs, as for sheep ER, led to two ER populations, one which significantly binds neither E_2 nor OHT (ligand-binding incompetent population) and the other which binds OHT with high affinity and E_2 with very low affinity (ligand-binding competent population).

The binding of the various ligands to this latter population generated upon DEPC treatment of wild-type and H524A ERs was studied through competition binding experiments, using [^{3}H]OHT as tracer. The variations in ligand RACs shown in Table 3 indicated that: (i) DEPC treatment of wild-type ER induced almost no change in RU and 17β-dE_2 affinities (<2-fold variation), a moderate change in Ral affinity (<4-fold decrease), and striking changes in E_2 (56-fold decrease) and probably 3-dE_2 affinities; (ii) H524A substitution greatly suppressed the ability of DEPC treatment to reduce E_2 affinity (only 3-fold decrease, as for 17β-dE_2) and abolished the effects of this treatment on RU and Ral affinities. These results strongly suggested that H524 is directly involved in the discriminating effects of DEPC on estrogen and antiestrogen recognition.

Ligand Protection against DEPC Inactivation of Wild-Type and Mutant ERs. Incubation of COS cell extracts, containing E_2- or OHT-bound ERs, with DEPC resulted in decreases in ligand-binding activities that were less pronounced than those corresponding to unliganded ERs. Note that this protection could just reflect a decrease in the ER inactivation rate, since this reagent has a short half-life

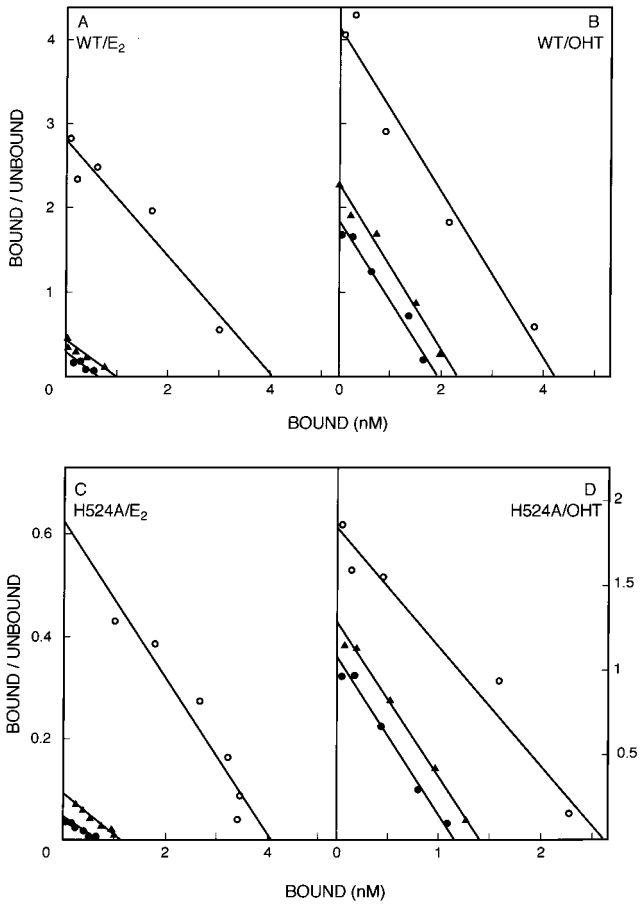

FIGURE 3: Saturation analysis of the binding of E_2 and OHT to control and DEPC-treated wild-type and H524A ERs. Portions of COS cell extracts containing wild-type or H524A ER were incubated for 30 min at 0 °C with 0, 2, or 4 mM DEPC. After histidine addition, aliquots of the various portions were incubated for 24 h at 0 °C with increasing concentrations of [^{3}H]E_2 or [^{3}H]-OHT in the absence and presence of 5 μM of the corresponding unlabeled ligand. Binding of labeled ligands was determined by charcoal assays. The specific binding of [^{3}H]E_2 and [^{3}H]OHT was calculated from the total concentration of labeled ligand (T) and concentrations of charcoal-resistant bound labeled ligand, measured in the presence (B_2) and absence (B_1) of unlabeled ligand, as described under Experimental Procedures. The concentration of unbound ligand was calculated as $T - B_1$. These values were then used for Scatchard representation of the specific binding of [^{3}H]E_2 (A and C) or [^{3}H]OHT (B and D) in control (○) and DEPC-treated (▲, 2 mM; ●, 4 mM) COS extracts containing either wild-type (A and B) or H524A (C and D) ER. Plots correspond to means of duplicate determinations. Data in panels C and D are from two different experiments. Linear regression from corresponding plots gave the following: panel A: (○) $K_A = 0.69 \times 10^9$ M^{-1}, $N = 4.0$ nM; (▲) $K_A = 0.43 \times 10^9$ M^{-1}, $N = 0.97$ nM; (●) $K_A = 0.43 \times 10^9$ M^{-1}, $N = 0.66$ nM; panel B: (○) $K_A = 0.97 \times 10^9$ M^{-1}, $N = 4.2$ nM; (▲) $K_A = 0.97 \times 10^9$ M^{-1}, $N = 2.3$ nM; (●) $K_A = 0.92 \times 10^9$ M^{-1}, $N = 2.0$ nM; panel C: (○) $K_A = 0.15 \times 10^9$ M^{-1}, $N = 4.1$ nM; (▲) $K_A = 0.082 \times 10^9$ M^{-1}, $N = 1.1$ nM; (●) $K_A = 0.067 \times 10^9$ M^{-1}, $N = 0.70$ nM; panel D: (○) $K_A = 0.71 \times 10^9$ M^{-1}, $N = 2.6$ nM; (▲) $K_A = 0.91 \times 10^9$ M^{-1}, $N = 1.4$ nM; (●) $K_A = 0.94 \times 10^9$ M^{-1}, $N = 1.2$ nM.

[probably <15 min at 0 °C, pH 7 (*28*)]. When occupied by OHT, wild-type (Figure 4A), H516A (Figure 4B), and H524A (Figure 4C) ERs were fully resistant to the action of DEPC concentrations up to 8 mM, the highest concentration tested. The protection role of E_2, used at saturating concentrations (as high as 80 nM for H524A ER), strongly depended upon the ER type. Wild-type and H516A ERs were efficiently protected against low reagent concentrations, but the protection efficiency decreased as the reagent concentra-

Table 3: Variation of Ligand RACs for Wild-Type and H524A ERs upon Modification by DEPC[a]

	RAC ratio	
ligand	WT	H524A
OHT	1	1
Ral	0.28 ± 0.11	1.0 ± 0.2
RU	0.79 ± 0.17	1.2 ± 0.3
E_2	0.018 ± 0.005	0.33 ± 0.11
3-dE_2	≪0.15	ND
17β-dE_2	1.47 ± 0.80	0.38 ± 0.06

[a] RACs of ligands for wild-type and H524A ERs, either native or pretreated with 4 mM DEPC, were determined as described under Experimental Procedures. Ratio of the RAC for DEPC-treated ER (wild-type and H524A ERs) to that for native ER was calculated for each of the five OHT competitors. Data given are means ± SD from at least 3 independent determinations. ND: not determined.

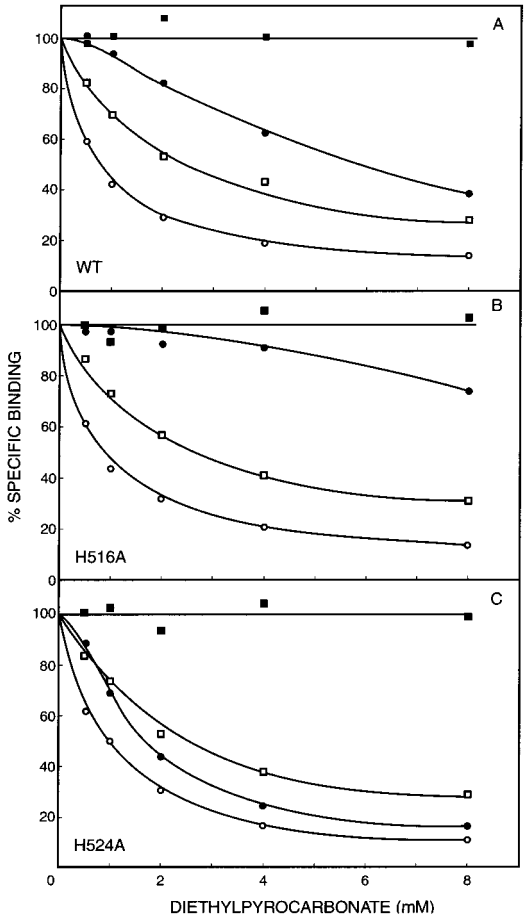

FIGURE 4: Inactivation of E_2 and OHT binding to wild-type, H516A, and H524A ERs by DEPC. Portions of COS cell extracts containing wild-type (A), H516A (B), or H524A (C) ER, incubated at 0 °C (prelabeled extracts) or not (unlabeled extracts) with saturating concentrations of [^{3}H]E_2 or [^{3}H]OHT, were treated with increasing DEPC concentrations for 30 min at 0 °C; they were then supplemented with histidine. Unlabeled aliquots were incubated at 0 °C with [^{3}H]E_2 or [^{3}H]OHT (postlabeled extracts). Binding of [^{3}H]E_2 or [^{3}H]OHT in the various aliquots was determined by charcoal assays. The specific binding of [^{3}H]E_2 (●, ○) and that of [^{3}H]OHT (■, □) in extracts are expressed as a percentage of the corresponding binding in extracts not treated by DEPC. Extracts prelabeled with [^{3}H]E_2 (●) or [^{3}H]OHT (■); extracts postlabeled with [^{3}H]E_2 (○) or [^{3}H]OHT (□). Values are means of duplicate determinations; experimental variation was under 15%.

tion increased: at 8 mM DEPC, ~40% and ~75% of the initial wild-type and H516A ER complexes were preserved, respectively. H524A ER was very poorly protected by E_2, even at low DEPC concentrations, with only ~15% of the initial complexes persisting at 8 mM reagent concentration. The partial protections exerted by E_2 on wild-type, H516A, and especially H524A ERs appeared to be intrinsic properties of ER/E_2 complexes and did not result from differences between E_2 and OHT affinities. Indeed the protection efficiencies were not improved when E_2 concentrations were boosted in order to decrease the dynamic portions of unliganded ER molecules (not shown).

DISCUSSION

Crystallographic data have shown that H524 of human ERα interacts with 17*β*/c-OH of estrogens or antiestrogens (*12*, *14*). In this study, we checked the involvement of H524 in the binding of six ER ligands displaying estrogenic or antiestrogenic properties and possessing or not 17*β*/c-OH. For this purpose, we substituted alanine for H524 and modified histidine residues with DEPC, and then determined the effects of these changes on ligand affinities.

The 42-fold difference found between the 17*β*-dE_2 RAC and that of 3-dE_2 for wild-type ER indicates that the contribution of 3-OH to E_2 binding is much stronger than that of 17*β*-OH, consistent with previous results (*29*). The very high affinity of OHT, which does not possess 17*β*/c-OH, together with the differential ligand binding properties of human and sheep ERs (*22*, *30*), emphasizes the subtle role of 17*β*/c-OH in ligand recognition properties and its possible interaction with H524. The H524A substitution did not change the RAC of 17*β*-dE_2, whereas those of E_2 and 3-dE_2 decreased 24-fold and 49-fold, respectively, the affinity of E_2 being surprisingly 9-fold lower than that of 17*β*-dE_2. These strong effects, not observed with the H516A mutant, underline the importance of H524 for the binding of estrogens possessing 17*β*-OH and highlight the negative contribution of this function for binding to H524A ER. For antiestrogens possessing 17*β*/c-OH, the H524A substitution induced less pronounced effects with some discrimination according to antiestrogen structure: while the RAC of Ral was 14-fold decreased, that of RU was only 3-fold lowered. The relative dissociation rates of E_2 and OHT from H524A ER agreed with their RACs, the dissociation rate of OHT itself being similar to that measured for wild-type ER; however, that of E_2 from wild-type ER did not accurately reflect its RAC.

The effect of DEPC on wild-type and mutant ERs was very similar to that previously observed using sheep uterine ER (*21*, *22*); the action of the reagent on each ER type led to two ER populations: a ligand-binding incompetent population which significantly binds neither E_2 nor OHT, and a ligand-binding competent population which displays high affinity for OHT and very low affinity for estrogens possessing 17*β*/c-OH. Although DEPC could modify various amino acid residues, we postulated that at low reagent/protein ratios and neutral pH the observed effects likely resulted from selective histidine residue modification. Mammalian ERα LBDs (including sheep and human) possess 13 histidine residues which are all conserved (*31*), while only 6 of them are conserved in human and rat ER*β* LBDs (*9*, *10*). According to crystallographic data (Figure 5), these six

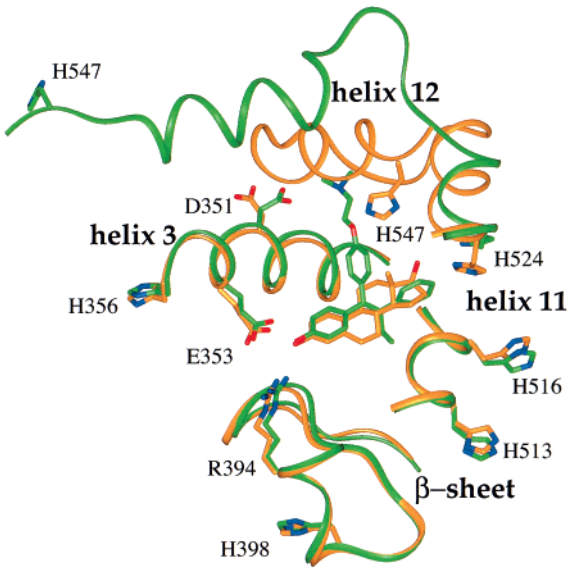

FIGURE 5: Spatial orientation of histidine residues located in the neighborhood of ER LBP. Crystallized LBD monomers (*12*, *14*) bound to E_2 (orange) or OHT (green) were superimposed using homologous helices and *β*-sheets. Portions of superimposed helices (numbers 3, 11, and 12) and *β*-sheets bearing the six histidine residues located near LBP are shown together with the relative configurations of the two LBD-bound ligands and those of the six histidine pairs: 356, 398, 513, 516, 524 (the latter involved in hydrogen bond with 17*β*-OH of E_2), and 547. Amino acid residue pairs involved in hydrogen bonding of the phenolic OH of ligands (E353 and R394) and in salt bridge with the amino group of OHT (D351) are represented.

histidine residues, i.e., H356 (helix 3); H398 (helix 6−*β*-sheet loop); H513, H516, and H524 (helix 11); and H547 (helix 12), are all localized within the vicinity of LBP, whereas the seven other histidine residues are more distant. It seems reasonable to suppose that histidine residues close to LBP should be primarily involved in the DEPC effects. In the conditions used, DEPC mainly induces carbethoxy monosubstitution at the NH of the histidine imidazole ring (*28*), which results in both steric hindrance and NH function blockade. As H547 is located on helix 12 which is not involved in LBP buildup, and DEPC treatment of H516A and H524A mutant ERs induced decreases in the number of binding sites similar to that observed for wild-type ER, we postulated that H516, H524, and H547 are not involved in generating the ligand-binding incompetent ER population. In crystallized ERα LBD complexes, H356 lies in close proximity to E353 (at 0.8 turn from the latter in helix 3), whereas H398 and H513 are spatially vicinal to R394 (Figure 5). Since E353 and R394 constitute the hydrogen-bonding anchorage site of the phenolic OH of E_2 and OHT, it is likely that DEPC modification involving one, or several, of the three above-mentioned histidine residues would preclude efficient binding of the two ligands. This effect might result from perturbation of local interaction networks involving histidine contacts with surrounding amino acids, or from direct perturbation of E353 and/or R394 interactions with E_2 or OHT. It could explain the complete loss of ligand binding by one of the DEPC-modified ER populations. The occurrence of the ligand-binding competent ER population upon DEPC action would result from a pattern of histidine modification that differs from that involved in generating the incompetent population. While this population displayed

almost unchanged RACs for RU and Ral, estrogens possessing 17β-OH were much more poorly recognized (56-fold decrease in E_2 affinity). Since the loss of estrogen affinity was no longer observed for the H524A mutant, we concluded that H524 was involved in DEPC generation of this specific ER population.

The partial and full blockades of the DEPC effects by E_2 and OHT, respectively, indicated that these ligands differently impeded reagent accessibility to histidine residues involved in the inactivation of unliganded ERs. The full protection of wild-type and mutant ERs by OHT suggested that histidine residues modified by the reagent are located either inside or in the neighborhood of LBP. The analysis of crystallized LBD/E_2 and LBD/OHT complexes did not highlight differences in histidine residue accessibility to DEPC: indeed, with the exception of H547, located in helix 12, which does not appear to be involved in the formation of the ligand-binding incompetent ER population, the six conserved histidine residues located close to LBP showed very similar locations and orientations (Figure 5). Inactivation of an ER/ligand complex is probably a multistage process in which several histidine residues could be progressively involved. Moreover, DEPC access to these residues would directly depend on the likely existence of various conformational states (as assessed by biphasic ligand dissociation kinetics), their interconversion rates, and the stabilities of intact or sequentially modified ER/ligand complexes. The protective effect of E_2 was modulated in opposite directions by H516A and H524A substitutions. Here again the likely existence of conformational multiplicities does not clearly indicate that these two histidine residues are DEPC targets. Future work dealing with mass spectrometry analysis of DEPC-modified ERs will provide an accurate determination of histidine modification patterns. Such experiments might provide a way to dissect interconversion between conformational states and its modulation by different estrogens and antiestrogens.

Taken together, the mutagenesis data and DEPC treatment experiments indicate that high-affinity binding of antiestrogens bearing 17β/c-OH is not predominantly governed by interaction of this function with H524. The weak relative contribution of this interaction might result from additional interactions of the antiestrogen aminoethoxyphenyl group with other amino acid residues, including D351 (*12*, *14*). To try to explain the higher insensitivity of RU binding to H524A substitution or DEPC-modification (as compared to E_2 and Ral), we built a model of the LBD/RU complex, for which no crystallographic structure is available. We used the crystallographic structure of the LBD/Ral complex (*12*) as a template for RU docking; then we submitted the complex to molecular dynamics simulations, to explore possible conformational states that would display substantially modified ligand positioning, as previously found for other ER ligands (*32*). These simulations did not allow us to find any conformational state of the complex, which no longer complied with the 17β-OH/H524 proximity, suggesting that the 17β/c-OH/H524 distance alone cannot account for the potential weakening of the RU 17β-OH/H524 interaction. Moreover, superimposition of complexes via quasi-invariant LBD helices led to close overlaps between docked RU and LBD-bound E_2 (Figure 6A), OHT (Figure 6B), and Ral (Figure 6C). The relative lack of importance of the RU 17β-OH/H524 interaction might be due to the presence of multiple conformational states; most of these states might not display the optimal geometry for the 17β-OH/H524 interaction and might not be accounted for by crystallographic data. Note that similar considerations about conformational multiplicity have been put forward to explain an unexpected crystallographic structure of a cysteine/serine ER mutant (*33*).

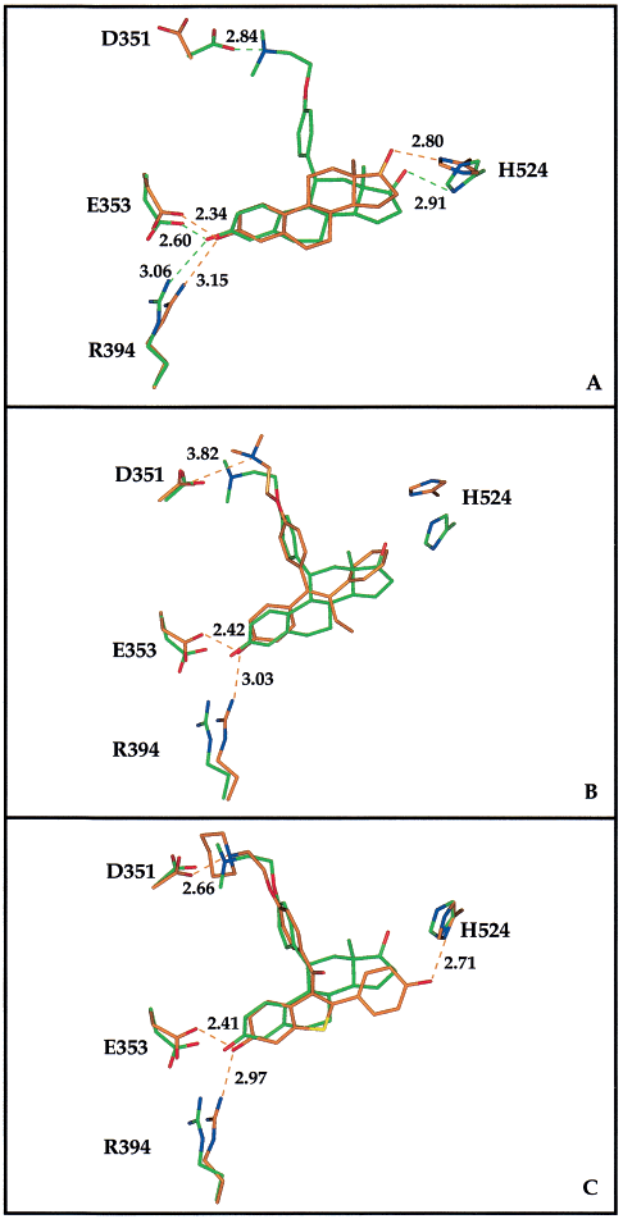

FIGURE 6: Overlap of docked RU with ER-bound E_2, OHT, and Ral. RU-containing LBD monomer, built as described under Experimental Procedures, was successively superimposed via homologous helices and β-sheets to crystallized LBD monomers bound to E_2, Ral (*12*), or OHT (*14*). Then LBD structures were deleted with the exception of side chains of (i) E353, R394 (involved in hydrogen bonding of E_2 and RU 3-OH or counterpart in Ral and OHT), (ii) H524 (involved in hydrogen bonding of E_2 and RU 17β-OH or counterpart in Ral), and (iii) D351 (involved in salt bridge formation with the amino group of OHT, Ral and RU). Overlaps of RU (green) with E_2, OHT, or Ral (orange) are shown in (A), (B), and (C), respectively; amino acid residues that make direct hydrogen or saline bonds (broken lines) with the ligands are shown in green (RU) or orange (E_2, OHT, and Ral); distances (Å) between interacting atoms of ligand and LBP amino acid residues are specified.

In summary, the approaches outlined in the present paper clearly highlight the differential interactions of 17β/c-OH of E_2, Ral, and RU with H524. Our results constitute a complement to previous results obtained by B. S. Katzenellenbogen's group. H524 appears to exert negligible or moderate roles on the binding and pharmacological properties of the various antagonists tested. It might be due to the existence of interactions of D351 with the 11β substituent (or equivalent for Ral) of these ligands. The importance of the latter interactions was underlined by modifications of ligand pharmacological properties upon substitution of this residue (*34*, *35*). Interestingly, residues located at nearly homologous positions in other receptors, e.g., the mineralocorticoid receptor (*36*), were shown to possess similar properties in controlling the balance between agonist or antagonist behavior of 11β-substituted synthetic ligands.

ACKNOWLEDGMENT

We are grateful to Benita Katzenellenbogen (University of Illinois) for donation of the plasmids coding for wild-type human ERα and H516A and H524A mutants and to François Nique (Aventis) for the gift of E_2, 3-dE_2, 17β-dE_2, and RU. We also thank Zeneca Pharmaceuticals and Lilly Research Laboratories for donations of OHT and Ral, respectively.

REFERENCES

1. Couse, J. F., and Korach, K. S. (1999) Estrogen receptor null mice: what we learned and where will they lead us? *Endocr. Rev. 20*, 358−417.
2. McGuire, W. L., Carbone, P. P., and Vollmer, E. P. (1975) *Estrogen receptors in human breast cancer*, Raven Press, New York.
3. Tsai, M. J., and O'Malley, B. W. (1994) Molecular mechanisms of action of steroid/thyroid receptor superfamily members. *Annu. Rev. Biochem. 63*, 451−486.
4. Mangelsdorf, D. J., Thummel, C., Beato, M., Herrlich, P., Schultz, G., Umesono, K., Blumberg, B., Kastner, P., Mark, M., Chambon, P., and Evans, R. M. (1995) The nuclear receptor superfamily: the second decade. *Cell 83*, 835−839.
5. Kuiper, G. G. J. M., Carlson, B., Grandien, K., Enmark, E., Häggblad, J., Nilsson, S., and Gustafsson, J. Å. (1997) Comparison of the ligand binding specificity and transcript tissue distribution of estrogen receptors α and β. *Endocrinology 138*, 863−870.
6. Lubhan, D. B., Moyer, J. S., Golding, T. S., Couse, J. F., Korach, K. S., and Smithies, O. (1993) Alteration of reproductive function but not prenatal sexual development after insertional disruption of the mouse estrogen receptor gene. *Proc. Natl. Acad. Sci. U.S.A. 90*, 11162−11166.
7. Green, S., Walter, P., Kumar, V., Krust, A., Bornert, J. M., Argos, P., and Chambon, P. (1986) Human œstrogen receptor cDNA: sequence, expression and homology to v-*erb*-A. *Nature 320*, 134−139.
8. Greene, G. L., Gilna, P., Waterfield, M., Baker, A., Hort, Y., and Shine, J. (1986) Sequence and expression of human estrogen receptor complementary DNA. *Science 231*, 1150−1154.
9. Mosselman, S., Polman, J., and Dijkema, R. (1996) ERβ: identification and characterization of a novel human estrogen receptor. *FEBS Lett. 392*, 49−53.
10. Kuiper, G. G. J. M., Enmark, E., Pelto-Huikko, M., Nilsson, S., and Gustafsson, J. Å. (1996) Cloning of a novel estrogen receptor expressed in rat prostate and ovary. *Proc. Natl. Acad. Sci. U.S.A. 93*, 5925−5930.
11. Egea, P. F., Klaholz, B. P., and Moras, D. (2000) Ligand-protein interactions in nuclear receptors of hormones. *FEBS Lett. 476*, 62−67.
12. Brzozowski, A. M., Pike, A. C. W., Dauter, Z., Hubbard, R. E., Bonn, T., Engström, O., Öhman, L., Greene, G. L., Gustafsson, J. Å., and Carlquist, M. (1997) Molecular basis of agonism and antagonism in the œstrogen receptor. *Nature 389*, 753−758.
13. Tanenbaum, D. M., Wang, Y., Williams, S. P., and Sigler, P. B. (1998) Crystallographic comparison of the estrogen and progesterone receptor's ligand binding domains. *Proc. Natl. Acad. Sci. U.S.A. 95*, 5998−6003.
14. Shiau, A. K., Barstad, D., Loria, P. M., Cheng, L., Kushner, P. J., Agard, D. A., and Greene, G. L. (1998) The structural basis of estrogen receptor/coactivator recognition and the antagonism of this interaction by tamoxifen. *Cell 95*, 927−937.
15. Eiler, S., Gangloff, M., Duclaud, S., Moras, D., and Ruff, M. (2001) Overexpression, purification and crystal structure of native ERα LBD. *Protein Expression Purif. 22*, 165−173.
16. Pike, A. C. W., Brzozowski, A. M., Hubbard, R. E., Bonn, T., Thorsell, A. G., Engström, O., Ljunggren, J., Gustafsson, J. Å., and Carlquist, M. (1999) Structure of the ligand-binding domain of œstrogen receptor beta in the presence of partial agonist and a full antagonist. *EMBO J. 18*, 4608−4618.
17. Pike, A. C. W., Brzozowski, A. M., Walton, J., Hubbard, R. E., Thorsell, A. G., Li, Y. L., Gustafsson, J. Å., and Carlquist, M. (2001) Structural insights into the mode of action of a pure antiestrogen. *Structure 9*, 145−153.
18. Wurtz, J. M., Bourguet, W., Renaud J. P., Vivat, V., Chambon, P., Moras, D., and Gronemeyer, H. (1996) A canonical structure for the ligand-binding domain of nuclear receptors. *Nat. Struct. Biol. 3*, 87−94.
19. Ekena, K., Weis, K. E., Katzenellenbogen, J. A., and Katzenellenbogen, B. S. (1996) Identification of amino acids in the hormone binding domain of the human estrogen receptor important for estrogen binding. *J. Biol. Chem. 271*, 20053−20059.
20. Ekena, K., Weis, K. E., Katzenellenbogen, J. A., and Katzenellenbogen, B. S. (1997) Different residues of the human estrogen receptor are involved in the recognition of structurally diverse estrogens and antiestrogens. *J. Biol. Chem. 272*, 5069−5075.
21. Borgna, J. L., and Scali, J. (1989) Differential inhibition of estrogen and antiestrogen binding to the estrogen receptor by diethylpyrocarbonte. *J. Steroid Biochem. 31*, 427−436.
22. Borgna, J. L., and Scali, J. (1991) Differential interactions of estrogens and antiestrogens at the 17β-hydroxy or counterpart function with the estrogen receptor. *Eur. J. Biochem. 199*, 575−585.
23. Bradford, M. M. (1976) A rapid and sensitive method for the quantitation of microgram quantities of protein utilizing the principle of protein dye binding. *Anal. Biochem. 72*, 248−254.
24. Blondeau, J. P., and Robel, P. (1975) Determination of protein−ligand binding constants at equilibrium in biological samples. *Eur. J. Biochem. 55*, 375−384.
25. Korenman, S. G. (1970) Relation between estrogen receptor inhibitory activity and binding to cytosol of rabbit and human uterus. *Endocrinology 87*, 1119−1123.
26. Salomonsson, M., Carlsson, B., and Häggblad, J. (1994) Equilibrium hormone binding to human estrogen receptors in highly diluted cell extracts is noncooperative and has a *Kd* of approximately 10 pM. *J. Steroid Biochem. Mol. Biol. 50*, 313−318.
27. Borgna, J. L., and Rochefort, H. (1980) High-affinity binding to the estrogen receptor of [^{3}H]4-hydoxytamoxifen. *Mol. Cell. Endocrinol. 20*, 71−85.
28. Miles, E. W. (1977) Modification of histidyl residues in proteins by diethylpyrocarbonate. *Methods Enzymol. 47*, 431−443.
29. Anstead, G. M., Carlson, K. E., and Katzenellenbogen, J. A. (1997) The estradiol pharmacophore: ligand structure-estrogen receptor binding affinity relationships and a model for the receptor binding site. *Steroids 62*, 268−303.
30. Aliau, S., Mattras, H., Richard, E., and Borgna, J. L. (1999) Cysteine 530 of the human estrogen receptor α is the main

covalent attachment site of 11β-(aziridinylalkoxyphenyl)-estradiols. *Biochemistry 38*, 14752−14762.
31. Madigou, T., Tiffoche, C., Lazennec, G., Pelletier, J., and Thieulant, M. L. (1996) The sheep estrogen receptor: cloning and regulation of expression in the hypothalamo-pituitary axis. *Mol. Cell. Endocrinol. 121*, 153−163.
32. Stauffer, S. R., Coletta, C. J., Tedesco, R., Nishiguchi, G., Carlson, K., Sun, J., Katzenellenbogen, B. S., and Katzenellenbogen, J. A. (2000) Pyrazole ligands: structure-affinity/activity relationships and estrogen receptor-α-selective agonists. *J. Med. Chem. 43*, 4934−4947.
33. Gangloff, M., Ruff, M., Eiler, S., Duclaud, S., Wurtz, J. M., and Moras, D. (2001) Crystal structure of a mutant hERα ligand-binding domain reveals key structural features for the mechanism of partial agonism. *J. Biol. Chem. 276*, 15059−15065.
34. Levenson, A. S., Catherino, W. M., and Jordan, V. C. (1997) Control of the estrogen-like actions of the tamoxifen-estrogen receptor complex by the surface amino acid at position 351. *J. Steroid Biochem. Mol. Biol. 60*, 261−268.
35. Webb, P., Nguyen, P., Valentine, C., Weatherman, R. V., Scalan, T. S., and Kushner, P. J. (2000) An antiestrogen-responsive estrogen receptor α mutant (D351Y) shows weak AF-2 activity in the presence of tamoxifen. *J. Biol. Chem. 275*, 37552−37558.
36. Auzou, G., Fagart, J., Souque, A., Hellal-Levy, C., Wurtz, J. M., Moras, D., and Rafestin-Oblin, M. E. (2000) A single amino acid mutation of Ala-773 in the mineralocorticoid receptor confers agonist properties to 11β-substituted spirolactones. *Mol. Pharmacol. 58*, 684−691.

BI0121914